8-2007

New Theoretical Considerations in Polymer Rheology: Elastic Breakdown of Chain Entanglement Network

Shi-Qing Wang
University of Akron Main Campus, swang@uakron.edu

Sham Ravindranath

Yangyang Wang

Pouyan Boukany

New theoretical considerations in polymer rheology: Elastic breakdown of chain entanglement network

Shi-Qing Wang,[a] Sham Ravindranath, Yangyang Wang, and Pouyan Boukany
Department of Polymer Science and Maurice Morton Institute of Polymer Science, University of Akron, Akron, Ohio 44325

(Received 28 February 2007; accepted 4 June 2007; published online 10 August 2007)

Recent experimental evidence has motivated us to present a set of new theoretical considerations and to provide a rationale for interpreting the intriguing flow phenomena observed in entangled polymer solutions and melts [P. Tapadia and S. Q. Wang, Phys. Rev. Lett. **96**, 016001 (2006); **96**, 196001 (2006); S. Q. Wang *et al.*, *ibid.* **97**, 187801 (2006)]. Three forces have been recognized to play important roles in controlling the response of a strained entanglement network. During flow, an intermolecular locking force f_{iml} arises and causes conformational deformation in each load-bearing strand between entanglements. The chain deformation builds up a retractive force f_{retract} within each strand. Chain entanglement prevails in quiescence because a given chain prefers to stay interpenetrating into other chains within its pervaded volume so as to enjoy maximum conformational entropy. Since each strand of length l_{ent} has entropy equal to k_BT, the disentanglement criterion is given by $f_{\mathrm{retract}} > f_{\mathrm{ent}} \sim k_BT/l_{\mathrm{ent}}$ in the case of interrupted deformation. This condition identifies f_{ent} as a cohesive force. Imbalance among these forces causes elastic breakdown of the entanglement network. For example, an entangled polymer yields during continuous deformation when the declining f_{iml} cannot sustain the elevated f_{retract}. This opposite trend of the two forces is at the core of the physics governing a "cohesive" breakdown at the yield point (i.e., the stress overshoot) in startup flow. Identifying the yield point as the point of force imbalance, we can also rationalize the recently observed striking scaling behavior associated with the yield point in continuous deformation of both shear and extension.
 [DOI: 10.1063/1.2753156]

I. INTRODUCTION

As viscoelastic materials, polymers exhibit a rich variety of nonlinear flow phenomena. Most polymers of interest are entangled. Nonlinear flow behavior of these polymers depends on how chain entanglement responds to external deformation.[1–3] Chain entanglements are the topological constraints arising from the intimate intertwining of long chainlike molecules with one another. In the absence of flow, the effect of chain entanglement manifests itself in the strong chain length dependence of the zero-shear viscosity η_0, the chain self-diffusion constant D_s, and in the rubbery relaxation behavior.

The journey to account for chain entanglement and predict its role in polymer flow began six decades ago when Green and Tobolsky first devised a transient network model.[4] Since this approach is inherently phenomenological, it cannot account for the $\eta_0 \sim M_w^{3.4}$ scaling with weigh-averaged molecular weight M_w. The first molecular insight came 25 years later in 1971, when de Gennes proposed the idea[5] of reptative chain motion in tubelike confinement to describe polymer diffusion and relaxation in the linear response regime. The elegant simplicity of the reptation model quickly received worldwide attention from the communities of polymer physics and rheology. Soon, a detailed tube theory was developed to provide a full description of polymer dynamics in both linear and nonlinear regimes.[6] Various versions have since been worked out to bring the theory into quantitative agreement with experiment on nonlinear flow behavior,[7] although several basic challenges to the tube theory remain unresolved and formidable even in linear viscoelastic regime. Being inherently a single-chain picture, the tube theory cannot properly account for many-body effects such as the effect of constraint release. More importantly, it perceives a primitive chain to be trapped in a tube analogous to a particle situated in a potential well of infinite height. In reality, as pointed out in Sec. IV, the barrier for a chain to jump out the "tube" is of finite height. Nonreptative mechanisms are competing with reptation modes, and the lifetimes of the caging constraint are finite and vary with length scales. These difficulties suggest consideration of the microscopic force-based polymer mode coupling approach, which appears to provide a self-consistent account of the effects of nonasymptotic processes on the linear viscoelastic properties of entangled polymer melts and solutions at finite degrees of polymerization.[8]

One of the key calculations of the Doi-Edwards (DE) tube model is its quantitative prediction[9] of stress relaxation behavior of entangled polymers after a step shear. The theory explains the fast nonlinear relaxation process based on the concept of chain retraction within a tube. Here the primitive chain was perceived to retract inside the tube on a scale of the Rouse relaxation time τ_R, with the entanglement network

[a]Author to whom correspondence should be addressed. Electronic mail: swang@uakron.edu

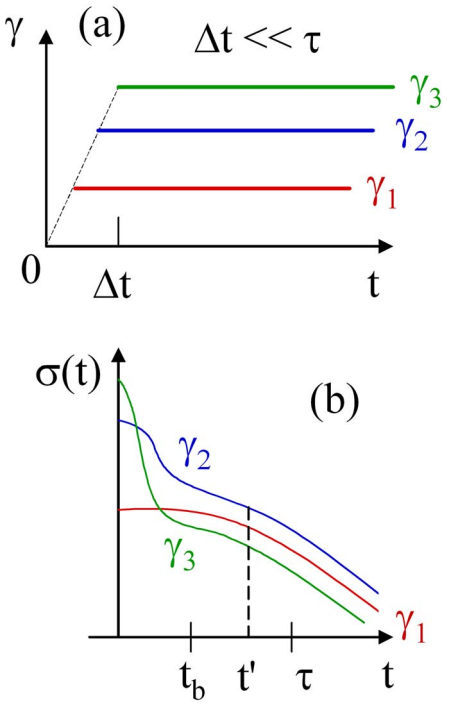

FIG. 1. (Color online) (a) Step shear at three amplitudes of γ_1 to γ_3, where "step" means a sudden imposition occurring over a very short time $\Delta t \ll t$. (b) The Doi-Edwards theory prediction, where the key feature is the kink, i.e., the rapid drop of the shear stress at a time designated by t_b, which is on the order of the Rouse relaxation time τ_R according to the theory. Beyond t_b, the time dependence is universal independent of the step amplitude. The quiescent terminal relaxation time, also known as the reptation time for monodisperse entangled polymers, is denoted by τ.

remaining intact after a large step strain. Under this explicit premise, the DE theory proceeds to calculate material functions such as relaxation modulus to depict the relaxation process. Figure 1 sketches the definition of step strain and the shear stress relaxation behavior for three respective amplitudes. The well-known quantitative agreement between one class of experimental data[10] and the DE theory[6] has been viewed as the most impressive evidence for the tube theory's ability to describe nonlinear flow behavior. Those step shear experiments (in agreement with the theory) have been known as *normal* type A behavior, where it was believed that the sample would relax *quiescently* after a step strain and the relaxation modulus could be a meaningful material function of the chain entanglement network. The most notable feature of both the type A behavior and the DE theory is that for different step strains, the relaxing shear stress σ decreases in quantitatively the same manner after a time t_b, independent of the amplitude of the applied strain γ, as illustrated in Fig. 1. In the superimposable time domain of $t > t_b$, a damping function h was introduced to depict the time-separability character of the type A relaxation behavior. Specifically, the damping function h normalizes the "relaxation modulus" $G(\gamma,t')$ at $t' > t_b$ by the relaxation modulus obtained in the linear regime: $h(\gamma)=G(\gamma,t')/G(\gamma \ll 1,t')$.

The DE theory prescribes that for $\gamma < 1$, h is nearly constant and for $\gamma > 2.3$, $h \sim \gamma^{-1.5}$, implying that the dimensionless shear stress $\bar{\sigma}(\gamma)=\sigma(t')/G(\gamma \ll 1,t')=h\gamma \sim \gamma^{-0.5}$ would decrease with the imposed strain γ for high values of γ, although it increases linearly with γ at low values of γ. As illustrated in Fig. 1, the theory predicts $\bar{\sigma}(\gamma_3) < \bar{\sigma}(\gamma_1)$, although $\gamma_3 > \gamma_1$, i.e., the shear stress at longer times ($t > t_b$) is lower for a larger applied step strain, due to the kinklike drop of the shear stress. Since only bonded retractive forces were considered in the calculation of the shear stress, the dip in the shear stress, as depicted in Fig. 1, is a natural consequence of chain retraction, through which local chain deformation quickly vanishes. On the experimental side, the seemingly similar kinklike stress drop was recently found to be associated with the occurrence of macroscopic motion after the step shear.[11] In other words, this surprising nonmonotonic function $\bar{\sigma}(\gamma)$ observed in experiment, which we would not expect without a structural breakdown of the entanglement network and went un-noticed in the popular form of the damping function h, actually appears to signal a cohesive or interfacial breakdown. A similar feature[6,12] of the DE theory, i.e., the predicted shear thinning viscosity $\eta \sim \dot{\gamma}^{-3/2}$ for $\dot{\gamma}\tau > 1$, shares the same origin as that of $h \sim \gamma^{-1.5}$. This feature would have also gone un-noticed had one not examined the nonmonotonic character of steady shear stress $\sigma = \eta\dot{\gamma} \sim \dot{\gamma}^{-1/2}$. Alarmingly, the nonmonotonic relationship of $\sigma(\dot{\gamma})$ with $\dot{\gamma}$ revealed in the original Doi-Edwards tube theory has been taken literally as indicating shear banding.[12] Since no shear banding was observed experimentally for entangled polymeric liquids as pointed explicitly in Ref. 7 and has only been reported in the literature since 2006,[13,14] in the past decade the theoretical efforts[15–19] have focused on removing the stress maximum by introducing such empirical ideas as convective constraint release.[20] We will return to this subject of stress maximum in Sec. II C.

Using an effective particle-tracking velocimetric (PTV) method, a recent experimental study[11] has explicitly revealed macroscopic motion inside entangled polybutadiene solutions after step shear. The macroscopic movement took place even though the sample experienced uniform deformation during the step strain. Apparently, it was the observed macroscopic movements in the sample interior that caused a rapid decline of the measured shear stress $\sigma(t)$ with time t, as depicted in Fig. 1. The magnitude of the macroscopic motion increases with the amplitude γ of the step strain, leading to steeper drop in σ and to a decreasing $\bar{\sigma}(\gamma)$ with γ at high values of γ. Thus, this PTV study of step shear indicated that the well-known agreement between theory and experiment was coincidental: The DE theory was devised to describe quiescent relaxation since it is not constructed to depict and does not anticipate any breakdown of chain entanglement network; the experimentally observed kinklike character in the relaxation modulus[6,9] was actually due to the substantial macroscopic motions after shear cessation.

In this paper, we are interested in exploring the universal physics governing both continuous and interrupted (more commonly known as step) deformations. Mounting experimental evidence challenges the basic understanding presently available in the literature and prompts us to search for a new theoretical framework to depict the experimental observations and to guide future experimental activities. The paper will be organized as follows. The following section, which the reader may choose to skip, provides a critical as-

sessment of the current theoretical pictures available on linear viscoelastic behavior of both nonentangled and entangled polymeric liquids. After a brief summary of new and surprising experimental findings on nonlinear behavior of entangled polymer solutions and melts, we will turn our main attention to a set of alternative ideas that redefines the theoretical tasks facing us.

In Sec. IV, we explore a new theoretical description of (well-entangled) polymer flow/deformation by focusing on a host of different questions from those raised previously: (a) whether the chain entanglement network is sufficiently fragile that it would actually disintegrate upon a sufficient external deformation, (b) what mechanism causes chain disentanglement after a large deformation, and (c) whether entangled polymers must first suffer yielding or breakup of the chain entanglement network before flow could take place during continuous deformation. Our recent experimental observations taught us that the matter of theoretically depicting entangled polymer flow must be addressed in two steps. The first-order issue is whether, when, and why chain entanglement would suffer catastrophic destruction. The second and somewhat remote task is to answer the question of how an entangled polymer flows after yielding, whether and how inhomogeneous shear and nonuniform extension would take place in macroscopic dimensions, and how such phenomena depend on the level of chain entanglement. At the present stage, we are merely concerned with learning something about the first-order issue.

In this present initial attempt, we have recognized three forces that play important roles in dictating the response of an entangled polymer to external deformation. Force imbalance has been perceived to take place among these forces either during or after an external deformation. At the center of this picture is the buildup of a (elastic) retraction force f_{retract} in each strand due to the imposed deformation. A sufficiently high f_{retract} can overcome the cohesion of the entanglement network, leading to its elastic breakup on time scales much shorter than the quiescent terminal relaxation time τ. The elastically induced chain disentanglement is expected to produce yielding in the form of nonquiescent relaxation after a large step strain, which has been indeed seen in experiment.[11] An explicit molecular picture is put forward to depict the various ingredients in this new theoretical picture at a single-chain level. Since behavior observed in any macroscopic experiment typically involves more than quadrillions (i.e., 10^{15}) of individual chains, any tractable theoretical modeling including the present under discussion can at best be expected to provide some useful guiding principles. In passing, we should also acknowledge the suggestion[21] that there may be material inhomogeneity and cooperative molecular motions beyond a single-chain scale in addition to the uniform background of chain entanglement, although direct experimental evidence has been difficult to establish. It is our judgment that the theoretical considerations presented here based on single-chain physics are directly applicable even in the presence of structural inhomogeneity because the elastic restoring force surely appears to be the source of the cohesive breakdown of the multichain structure.

II. ASSESSMENT ON CURRENT THEORETICAL UNDERSTANDING OF LINEAR VISCOELASTIC BEHAVIOR

Theoretical understanding of linear viscoelastic properties of polymeric liquids is still under active development despite constant modification of the Doi-Edwards tube model over the past three decades. In contrast, the experimental side of the picture is rather clear as far as linear responses are concerned. A very recent experiment[22] appears to challenge this impression as well and questions the familiar notion of linear viscoelasticity (LVE) of amorphous liquids. Thus, there are a number of unresolved theoretical questions, some brought up by recent experiments and computer simulations and others are themselves conceptually enticing to explore. We would like to selectively address them in three subsections as follows.

A. Single-chain versus interactive/colletive phases in "terminal" regime

Both the Maxwell phenomenological (spring-dashpot) model and subsequent molecular theories of Rouse and Zimm for dilute polymer solutions and Doi-Edwards for entangled polymer solutions and melts prescribe the existence of terminal flow behavior. In other words, these liquids at a temperature well above their glass transition temperatures are expected to flow and show characteristic terminal behavior at sufficiently long times as revealed in small amplitude oscillatory shear (SAOS) measurements, where the storage and loss moduli G' and G'' scale with the oscillation frequency ω as ω^2 and ω^1, respectively, in the limit of vanishingly low ω.

A recent experimental study[22] revealed finite frequency-independent G' at low frequencies for several nonentangled polymer melts, where a standard SAOS measurement would only disclose terminal behavior with $G' \sim \omega^2$. Using the same fixtures provided by the authors of Ref. 22 to assure optimal polymer adsorption, we have now also observed the emergence of such an unexpected solidlike response of a nonentangled liquid [poly(*n*-butyl acrylate)] at sufficiently small linear displacement of the moving surface in a parallel-disk shear cell. The yet-unknown large-scale structures responsible for the observed elasticity were so fragile that great care was required to allow long-time healing of the damaged sample that resulted during loading. It remains unknown whether the unexpected phenomenon would take place in other polymeric liquids. Currently, a host of questions remain highly elusive: what and how large structures would form collectively from individual molecules, whether and how the elastic behavior depends on the chain length, and whether the fragile "granular" structure is sensitive to temperature, i.e., whether there is a thermodynamic origin of these structures.

We are currently searching for nonrheological evidence of such previously unknown elasticity in low molecular-weight polymeric liquids using a method that would not introduce any mechanical deformation. Self-diffusion measurements by pulse-gradient NMR spin echo are one of the future studies to be carried out. Finally, in passing, we noted that

although the theoretical picture concerning material inhomogeneity is far from clear, some semiempirical considerations have been made to remind us of a broader viewpoint on polymer dynamics beyond single-chain models.[21]

Indeed, the classical Rouse model is based on a single-chain depiction[23] that calculates the bonded forces. In reality, nonbonded interchain interactions must also be taken into account for unentangled melts. We do not know of any mechanism via which nonbonded forces would allow short-chain melts to form dynamic clusters. On the other hand, nonbonded interchain interactions may depend sensitively on external deformation that perturbs the chain conformation, leading to shear thinning as observed experimentally,[24] although the standard Rouse model predicts no shear thinning.

B. Various models for chain entanglement

1. Onset entanglement molecular weight M_e determined from linear viscoelasticity

The effects of chain entanglement have been recognized for a long time.[1,2] In particular, chain entanglement apparently makes the polymer respond like a rubbery network in the sense that it can display an elastic stress plateau over a wide range of time scales in either SAOS or stress relaxation after a small step strain. A heuristic picture to depict how chain entanglement affects diffusion and terminal relaxation processes is due to de Gennes[5] who perceived a primitive chain to reptate in an imaginary rigid tube made of other chains. However, this model itself does not probe the questions of how chain entanglement arises in a liquid composed of linear long chainlike molecules and what the minimum chain length must be for the liquid to exhibit elastic characteristics in SAOS measurements.

In either a tube model of Doi-Edwards or the classical rubber network theory for entangled polymers, the elastic plateau modulus G_p due to chain entanglement is explicitly inversely proportional to the molecular weight $M_e(\phi)$ between neighboring entanglement points,

$$G_p(\phi) = \theta k_B T, \tag{1}$$

where the number density θ of entangling strands is given by

$$\theta = \phi[\rho N_a / M_e(\phi)]. \tag{2}$$

Here ϕ is the volume fraction of polymer that would be unity for melts and less than unity for solutions, ρ the mass density, and N_a the Avogadro constant.

In the LVE limit, the polymer flow behavior is described by a linear relationship between stress σ and shear or extension rate $\dot{\gamma}$ or $\dot{\varepsilon}$. The proportionality constant is the zero-shear viscosity $\eta_0 \sim G_p \tau$ for shear flow and $\eta_{e0} = 3\eta_0$ for extensional flow. The self-diffusion behavior (in quiescence) might be related to η_0 through the coil size R_g as $D_s \approx G_p R_g^2 / \eta_0$ only in the asymptotic limit of infinite chain length. For modestly high values of M/M_e, the scaling behavior of $D_s \sim M_W^{-2.4}$ for entangled polymers deviates from the ideal reptation scaling of M_W^{-2} due to the acceleration of the asymptotic diffusion behavior by some constraint release effect.[25]

Thus, another way to empirically identify entanglement is to measure either the zero-shear viscosity η_0 or the self-diffusion constant D_s and determine at what value of M_c the scaling behavior of such properties changes from M_w and M_w^{-1} to $M_w^{3.4}$ and $M_w^{-2.4}$, respectively (under approximate iso-free volume condition). However, it has been noted[26] that M_c determined from the borderline separating the different scaling laws is different from M_e obtained from the plateau modulus G_p. This discrepancy, if confirmed, would imply that different physical processes have different onset conditions for entanglement.

2. Chain entanglement models

Attempts have been made in the recent decades to explore the origin of chain entanglement. Since chain entanglement manifests itself in different ways, various definitions and accounts of chain entanglement emerged in the literature. Despite a recent critical review on the subject,[27] confusion remains in the task to reconcile the different accounts of onset entanglement molecular weight M_e. In the packing model,[28–31] it is perceived that chain entanglement occurs in a monodisperse melt of molecular weight M when enough interchain topological intertwining builds up as M increases. As the volume of $\Omega = (4\pi/3)R_g^3$ pervaded by a chain increases with the radius of gyration R_g, the number Q of chains required to fill it up increases according to $Q = \Omega / v$, where v is the reciprocal of the chain number density $(\rho N_a / M)$, i.e., the physical volume per chain. For Gaussian chains, $Q \sim M^{1/2}$. Sufficient topological interchain interference occurs to form entanglement when Q increases to Q_e. The conjecture[28,29] is that Q_e is universal independent of chemical details. Indeed, for all polymers under study of different microchemical structures, Q_e appears to be a universal constant[32] around 5–6, where M_e is measured from the elastic plateau modulus, as delineated in Eqs. (1) and (2).

Starting from a completely different standpoint, the percolation model[33] sought to define chain entanglement by considering its mechanical consequences. Entanglement would arise to bear load when a chain is able to make a couple of loops across a flat surface. It is straightforward to estimate that the number q of times a chain passes through a loading-bearing surface is, on the average, $q = \pi R_g^2 / sQ$, where s is an effective averaged segmental cross-section area and Q has been defined in the preceding paragraph as the number of chains filling a volume pervaded by the chain. It was asserted that M_c corresponds to having $q_c = 3$ for all entangled flexible polymers. For Gaussian chains, $qQ \sim R_g^2 \sim M$, and therefore, analogous to Q, this number q also scales like $M^{1/2}$. Moreover, we find $Q/q = (4\pi/81)(s/p^2)$ to be independent of the chain length N, where p is a characteristic packing length that can be meaningfully defined only for Gaussian chains as[28] $6pR_g^2 = v = M/\rho N_a$ so that it is independent of M and depends only on the chemical structures of the monomer.

A recently completed reexamination[34] of this subject has, in our judgment, clearly indicated what model agrees much better with experimental data and what molecular characteristics dictate the onset of chain entanglement in terms of M_e. In particular, it is possible to draw generic conclusions.

Specifically, the following trends can be observed with few exceptions. (A) Most flexible polymers have nearly the same coil size for a given number of backbone bonds. (B) Chain entanglement occurs apparently when a given chain is surrounded by sufficient number of other chains. (C) It is the bulkiness of the chain segment that determines M_e. Entanglement occurs at a higher polymerization index n_e for bulkier chains, corresponding typically to a higher value of M_e.

C. Stress due to bonded versus nonbonded forces

The prevailing molecular theory for linear viscoelasticity of entangled polymers is widely considered to be that of the Doi-Edward tube model due to its simplicity. Following the early tradition of the rubber elasticity theory of James and Guth,[35] in the DE-type tube model, only bonded forces of the primitive chain are included in the evaluation of macroscopic stress. External deformation produces chain orientation, resulting in a finite stress from the resistance of the chain against the conformational entropy loss. After an instantaneous small amplitude step strain, the deformed chain, however, slightly, will retain a finite amount of bonded forces until it has returned to its equilibrium conformations on the terminal relaxation time scale τ. The stresses due to the bonded forces would not vanish in times much shorter than τ because the nonbonded forces maintain the chain deformation. Since an analytical description of how nonbonded forces produce chain deformation is rather intractable, one has to design other ways to depict molecular deformation due to external macroscopic deformation. In either the classical rubber elasticity theory or the tube model, the effect of nonbonded forces to produce chain deformation is accounted for by assuming that a given chain would undergo affine deformation.[7] In other words, the tube model is phenomenological and not formulated at the level of forces.

Actually, nonbonded forces, including intrachain excluded volume interactions and all interchain forces, have long been recognized to be part of the whole picture of polymer dynamics.[36,37] For the linear (small strain) viscoelastic behavior of well-entangled polymer melts, we may assume that bonded forces are completely balanced by the nonbonded forces in some time-averaged sense during and after external deformation. Thus, it may indeed suffice to adopt the simple scheme of only including the contributions of bonded force in an evaluation of stress relaxation after a small step strain. Some computer simulations have indicated that the nonbonded forces are more dominant[38,39] for stress relaxation. For small strains where a well-entangled polymer network is not expected to experience any breakdown in the sense of chain disentanglement, we reiterate that the two types of forces should remain balanced. For weakly entangled systems that were studied in the simulations, the implication of the simulation results is not obvious.

In the tube model only bonded forces can be calculated according to a prescribed flow condition. When chain disentanglement occurs at a point of imbalance between bonded and nonbonded forces, it may not be sufficient to calculate stresses from bonded forces alone. Recent and ongoing PTV observations[13,14,40] reveal that upon a so-called startup shear in the stress plateau region, well-entangled polymers indeed undergo homogeneous flow only *initially*, and then the shear stress passes a maximum before declining to a steady state. Inhomogeneous shear sets in after the stress overshoot and stabilizes as the shear stress attains its steady state value[40] where nonbonded forces could make a significant contribution. The cause of shear banding as a yielding process is the main topic of this work.

Due to the nonbonded forces, the actual rheometric measurements always produce a positive slope in the relation between the shear stress σ and the nominal shear rate V/H in steady state. In contrast, the Doi-Edwards tube theory predicts an unphysical maximum of the shear stress versus the applied shear rate in steady state.[6,12] In describing a startup shear, shear stress overshoot occurred[12] because its calculation contained only contributions from bonded forces, which drops upon chain retraction.[41] In other words, chain stretching and corresponding bonded forces are greatly reduced in steady state after chain retraction, leading to a sharp drop of the calculated shear stress. In the DE theory, the steady state shear stress σ is lower at a higher shear rate of V/H because the increased chain orientation in flow due to the tube alignment causes a decrease in the amount of bonded forces.[7,42] The end result is a negative slope in a plot of σ versus V/H. Thus, the well-known nonmonotonic constitutive relationship of the original Doi-Edwards theory[12] is due to the theoretical failure to include effects of nonbonded forces and to the artificial tube alignment that reduces the effectiveness of chain stretch by the external deformation. Clearly, this stress maximum feature of the original DE theory must not be taken as predicting shear banding. On the contrary, if shear banding occurs, one must first investigate the onset condition for what determines the onset of yielding and how chain disentanglement takes place to produce shear banding. We will return to this subject at the end of Sec. IV C.

III. NEW EXPERIMENTAL OBSERVATIONS CONCERNING NONLINEAR BEHAVIOR

Here we summarize key results from two types of experiments involving either step or continuous deformation. These experiments have provided invaluable insight into the actual physical picture of entangled polymer flow and formed the conceptual foundation of a new theoretical framework to be presented in the following section. Conversely, new theoretical concepts are required to delineate molecular mechanisms behind the intriguing and unexpected phenomena reviewed in this section.

A. Cohesive collapse after step shear and step extension

Step strain experiments have been carried out in both simple shear[11,43] and uniaxial extension.[44] These step strain experiments employ rates of deformation that are much higher than the terminal relaxation rate $1/\tau$. Our particle-tracking velocimetric observations on a family of entangled polybutadiene solutions reveal nonquiescent relaxation after a large step shear.[11] It is this elastic recoil-like macroscopic

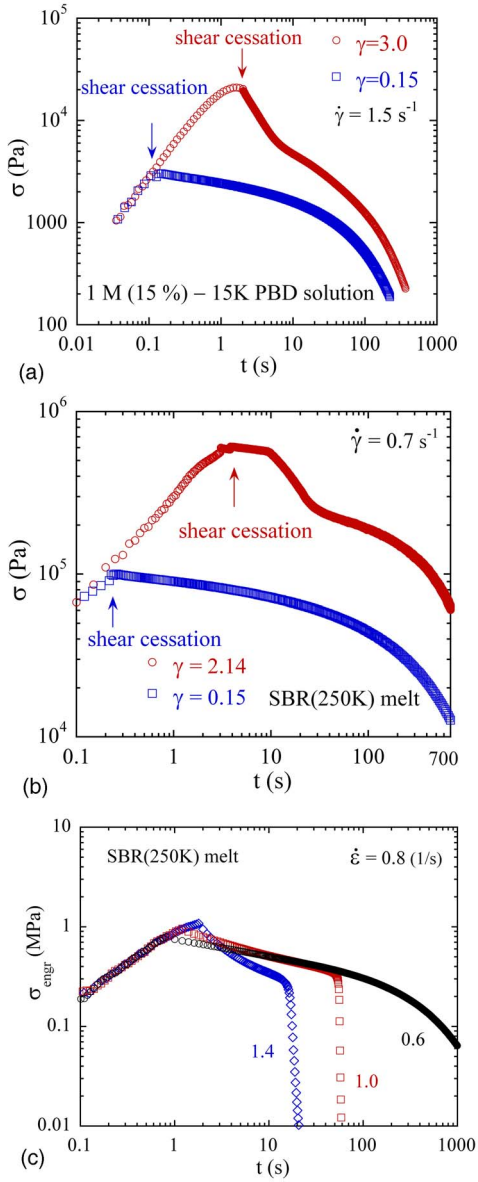

FIG. 2. (Color online) (a) Shear stress relaxation of a monodisperse 15% PBD solution (τ=83 s, τ_R=1.3 s) after strains of 0.15 and 3.0, where the number of entanglements per chain, Z, is around 66. (b) Shear stress relaxation of a monodisperse SBR melt (τ=310 s, τ_R=4.1 s) after strains of 0.15 and 3.0, where the number of entanglements per chain, Z, is around 76. (c) Step strain extension experiments involving amplitudes of ε=0.6, 1.0, and 1.4. The specimen remains uniform, i.e., intact for ε=0.6. However, higher amplitudes of step strain produce samples that are only temporarily stable. A subsequent breakup causes a sharp decline in the measured force.

internal motion that led to a rapid drop of the residual shear stress at γ=3, as seen in Fig. 2(a). Specifically, the critical strain that produces the macroscopic motion after shear cessation is as low as 140%, making it ill defined to perform measurement of a relaxation modulus beyond γ_c=1.4 and to compare with the Doi-Edwards tube theory. More recently,[45] step shear deformation has been seen for the first time to produce internal macroscopic motion in monodisperse entangled melts of styrene-butadiene rubber (SBR). A typical stress decay is shown in Fig. 2(b). Interestingly, the macroscopic motion was initially insignificant and built up after many seconds in this case of modestly step-sheared melt.

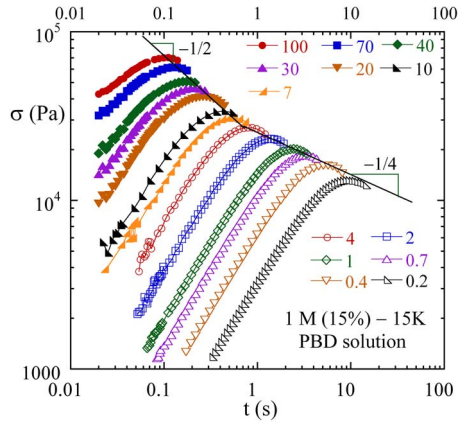

FIG. 3. (Color online) Shear stress growth as a function of time for various applied shear rates for the same 15% PBD solution, as described in Fig. 2(a), where the numbers indicate the shear rates in the unit of s^{-1}.

Analogously, when an entangled melt (SBR) is uniaxially stretched at a high rate ($\dot{\varepsilon}\tau \gg 1$) beyond a critical Hencky strain ε_c=0.8, the deformed specimen can no longer maintain its dimensional integrity and breaks apart over a time scale shorter than its terminal relaxation time τ. The breakup naturally produces a sharp drop in the tensile force, which occurs on time scales that can be much longer than the Rouse relaxation time τ_R and accelerates with increasing amplitude of the applied strain, as shown in Fig. 2(c). Analogous to the case of step shear experiments on entangled solutions of various degrees of chain entanglement,[11] this critical condition for breakup during relaxation was found to be the same, independent of the SBR's M_w ranging from 100 to 500 kg/mol.[44]

B. Yielding during continuous deformation

At high rates of startup shear with $\dot{\gamma}\tau > 1$, an entangled polymer would respond by showing a shear stress maximum, in contrast with the monotonic stress growth toward a steady state value, observed for $\dot{\gamma}\tau < 1$. The stress overshoot in the startup shear of entangled liquids has been known for decades.[46–50] This phenomenon resembles yielding behavior in deformation of plastics and glasses. Clearly, the initial elastic deformation cannot persist to indefinitely high strains beyond a stress level higher than the cohesive strength of the material. The solidlike response of the material is to yield structurally or cohesively, leading to a drop in the measured stress. Our particle-tracking velocimetric observations have shown that inhomogeneous shear quickly developed beyond the shear stress maximum in entangled polybutadiene (PBD) solutions[13,14] and SBR melts.[45] Figure 3 shows the shear stress growth[51] of a highly entangled 15% polybutadiene solution at different imposed rates of shear. It is worth noting that homogeneous shear prevails during such startup shear until the overshoot of time t_{max}, where the imposed strain $\gamma_y = \dot{\gamma} t_{max}$ has far exceeded γ_c=1.4. Since t_{max} is actually considerably shorter than the Rouse relaxation time (τ_R=1.3 s) of this sample for any applied rate higher than 2 s^{-1}, the sample as an entanglement network must be un-

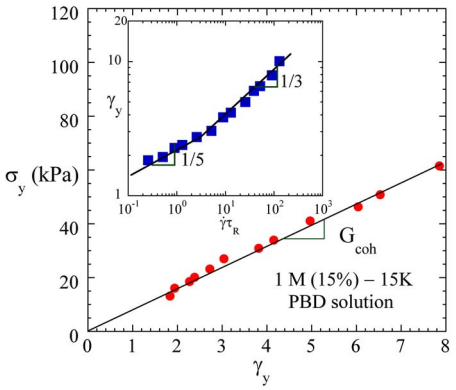

FIG. 4. (Color online) The peak shear stress σ_y as a function of the strain γ_y at the overshoot point, read from Fig. 3. The inset shows the dependence of the coordinate γ_y of the yield point on $\dot{\gamma}$, revealing an exponent of 1/3 for $\dot{\gamma}\tau_R > 1$.

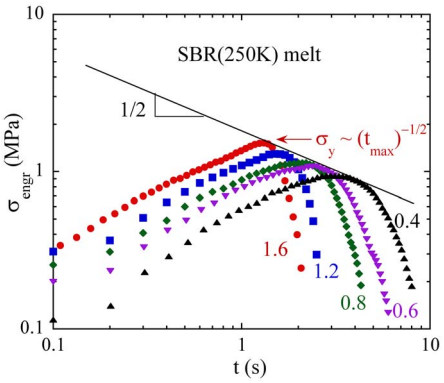

FIG. 5. (Color online) The measured tensile force resulting from five discrete continuous uniaxial stretching experiments, expressed in the form of the engineering stress σ_{engr}, where the numbers 0.4–1.6 s^{-1} indicates the Hencky rate of extension $\dot{\varepsilon}$.

dergoing elastic deformation up to the overshoot. The decrease of σ with further shearing is due to yielding of the material.

We regard the stress overshoot as a yield point and denote the coordinates of the shear stress maximum as (γ_y, σ_y). Upon analyzing Fig. 3 in detail, we found scaling behavior associated with the characteristics of the yield point.[52] Figure 4 reveals that the maximum shear stress σ_y is exactly a linear function of the yield strain γ_y at the maximum, where the inset indicates that the yield strain γ_y scales with the applied rate as $\dot{\gamma}^{1/3}$, provided that $\dot{\gamma}\tau_R > 1$.

More recently, we have carried out parallel studies of continuous extension on a series of monodisperse entangled SBR melts.[44,53] When the applied rate of extension $\dot{\varepsilon}$ is higher than the reciprocal relaxation time τ, i.e., $\dot{\varepsilon}\tau > 1$, a tensile force maximum is encountered,[51] beyond which the specimens undergo nonuniform extension. A strikingly similar set of scaling results was found for extensional deformation of SBR melts.[44] For example, Fig. 5 shows the emergence of the tensile force maxima at different rates of extension for a monodisperse SBR melt of $M_w = 250$ kg/mol, where $\sigma_y \sim (t_{max})^{-1/2}$ for $\dot{\gamma}\tau_R > 1$, which is the same as seen in Fig. 3.

IV. NEW THEORETICAL PICTURE IN NONLINEAR POLYMER RHEOLOGY: CHAIN DISENTANGLEMENT, FORCE IMBALANCE, AND ELASTIC BREAKUP

The experimental observations briefly described in Sec. III have provided crucial insight into the nature of well-entangled polymer flow. Conversely, the results from step and continuous deformation experiments are rather unexpected and even counterintuitive because they challenge the established perception of flow behavior of entangled polymers. Clearly, new ingredients are required in a more realistic theoretical depiction of the observed phenomena. The main purpose of this work is to identify these building blocks and present a different theoretical framework that is consistent with the available experimental observations and can guide us to uncover new unexpected phenomena.

A. Step shear: Overcoming entanglement cohesion

As mentioned earlier, we found that a step-sheared sample would display *internal* macroscopic motion *after* shear cessation when the applied strain amplitude γ is above $\gamma_c \sim 1.4$ for entangled solutions and melts. In parallel, the step extension experiments on entangled melts revealed similar yielding behavior after a critical strain $\varepsilon_c \sim 0.8$. Since chain entanglement is responsible for the cohesive integrity on time scales shorter than the terminal relaxation (reptation) time τ, the structural breakdown leading to macroscopic flow is plausibly a result of chain disentanglement. Importantly, this failure of entanglement network after a step deformation has been found to occur not only in entangled solutions but also in melts in both shear[45] and extension.[44]

1. Retraction force $f_{retract}$

In order to discuss the cause of the "cohesive" breakdown after step deformation, it is necessary to quantify the familiar consequence of an imposed deformation. Upon instant deformation of sufficient amplitude, each chain suffers conformational deformation. A strained chain would resist this deformation in the form of a retraction force $f_{retract}$. For entangled polymeric liquids, it is more straightforward to consider the retraction (bonded) force $f_{retract}$ per Gaussian strand between two neighboring entanglement points. The total force Σ measured from a sample area of A_0 in a macroscopic experiment comes from resistances of all such strands that have undergone deformation. Suppose that there are a total number of Φ entanglement strands passing across the area A_0. Taking simple shear, for example, we can relate the ensemble-averaged $f_{retract}$ to the amplitude γ of the instant step strain in terms of a shear modulus G as

$$\Sigma = \Phi f_{retract} = A_0 G \gamma, \tag{3}$$

where the number of strands per unit area Φ/A_0 is given by

$$\Phi/A_0 \approx \phi\rho[N_a/M_e(\phi)]l_{ent}(\phi), \tag{4}$$

with the mesh size or entanglement spacing $l_{ent}(\phi) \sim R_g[M_e(\phi)/M]^{1/2}$ and ϕ being unity for melts and the volume (or weight) fraction for solutions. For our purpose, it suffices to use the elastic plateau modulus G_p in Eq. (1). For

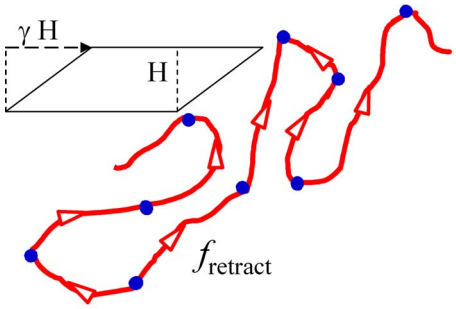

FIG. 6. (Color online) Production of retraction forces in each strand between entanglements due to chain deformation by the externally imposed strain. On the average, the retraction force $f_{retract}$ within a strand is proportional to the external shear strain γ for affine deformation.

a polymer solution of volume fraction ϕ, we have[54,55]

$$G_p(\phi) = G_N^0 \phi[M_e/M_e(\phi)], \tag{5}$$

with the pure melt's plateau modulus $G_N^0 \sim \rho k_B T N_a / M_e$, so that $G_p(\phi=1)=G_N^0$. Due to chain entanglement, the bonded $f_{retract}$ would not decrease much on time scales shorter than τ and can be estimated by inserting Eqs. (4) and (5) into Eq. (3),

$$f_{retract}(\gamma) \approx (k_B T/l_{ent})\gamma. \tag{6}$$

This elastic force $f_{retract}$ originates from the strand's resistance against deformation away from its isotropic equilibrium conformations. For an instant step (uniaxial) extension, $f_{retract}$ can be similarly derived in the spirit of the classical rubber elasticity theory. Figure 6 illustrates the retraction forces along a test chain due to a sudden simple shear strain γ.

2. Entanglement network in quiescence

Let us imagine immersing a long test chain among other chains of equal length. It appears that this test chain becomes localized when it is surrounded in its pervaded volume Ω by a sufficient number of the other chains, as indicated by the packing model.[28] All the chains enjoy maximum conformational entropy by interpenetrating and thus getting into each other's way, leading to the topological localization. The strength of the localization increases strongly with the chain length N or the number of entanglements per chain, $Z=N/N_e$. The test chain can be perceived to be pinned down at a number Z of entanglement points, as denoted by the open circles in Fig. 7. The chain entanglement prevails in quiescence because the test and surrounding chains are constantly interpenetrating. For each strand trapped between entanglement points, we assign a k_BT of conformational entropy, as shown in Fig. 7. The tube model was predicated on confinement of the test chain in a permanent tube. In the language of Fig. 7, the tube model treated the entanglement points as infinitely strong and permanent, at least in quiescence.

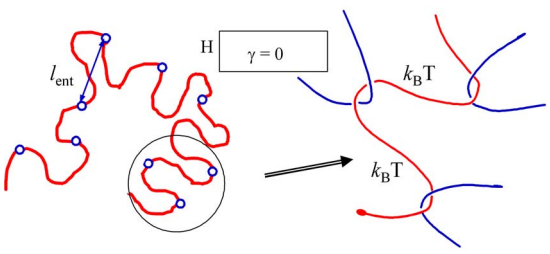

FIG. 7. (Color online) In quiescence, each Gaussian strand enjoys maximum conformational entropy on the order of k_BT by remaining hooked (i.e., immersed) with other chains.

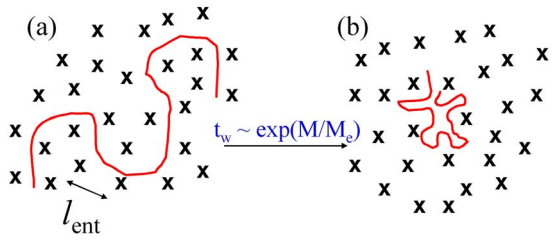

FIG. 8. (Color online) For a coiled chain to change from conformation (a) to (b) would require a waiting time proportional to $\exp(M/M_e)$, typically much longer than the reptation time τ for $M/M_e \gg 1$. Thus, reptation dynamics are dominant in quiescence.

We argue that it would cost k_BT to liberate one entanglement strand. In other words, a strand must sacrifice its favorable conformations to avoid intertwining with other chains. The probability to escape from the "tube confinement," if perceived as an Eyring activation process,[56] would be exponentially small, in quiescence, proportional to $\exp(-Z)$ for a linear chain of Z entanglement points. As visualized in Fig. 8, the waiting time for a chain to assume the conformation (b) by avoiding entanglement with surrounding chains increases exponentially with Z. Actually, the depiction of hypothetical disentanglement in Fig. 8 is reminiscent of the description[6,57] of arm retraction dynamics of branched chains in mutual entanglement. Since the delocalization probability, $\exp(-Z)$, is quite small for $Z \gg 1$, the reptation mode may indeed prevail to govern linear viscoelasticity of entangled polymers. On the other hand, for moderately entangled systems, other nonreptative processes (e.g., constraint release and contour length fluctuations) become more relevant.

3. Chain disentanglement after large step strain

In the absence of any external deformation, it is improbable for a Gaussian random coil to collapse onto itself so as to free itself from entanglement with others, as illustrated in Fig. 8. On the other hand, the entanglement points may be much more fragile than have been previously recognized. Since there is k_BT of energy associated with each strand in quiescence, there is a cohesive force of magnitude,

$$f_{ent} = k_B T/l_{ent}, \tag{7}$$

per entanglement that keeps the network intact on time scales shorter than the terminal relaxation time τ. This virtual force is clearly nonbonded and interchain in origin. Once again, analogous to the introduction of Eq. (6), f_{ent} in Eq. (7) can be more precisely taken as an ensemble-average quantity. When a sudden external strain produces affine chain deformation and a corresponding retraction force in each strand, as discussed in Eq. (6) and Fig. 6 of the preceding subsection, the elastic restoring force can be higher than the cohesive force

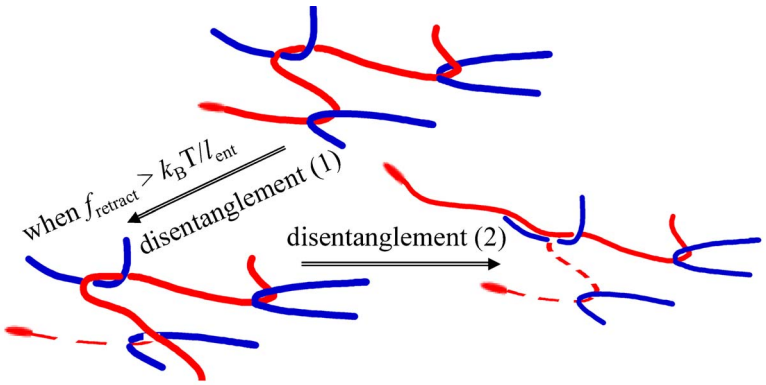

FIG. 9. (Color online) Depiction of sequential disappearance of entanglement points after a large imposed deformation from the chain ends (with filled dots). Depending on how many strands straighten, there will be one, two, or more (not depicted) entanglement points eradicated by the retraction force $f_{retract}$. The coils (dashed lines) at the entanglement junction(s) undergo straightening (i.e., to become the solid lines) when the available $f_{retract}$ in each strand is sufficiently high such that $f_{retract}l_{ent} > k_BT$.

of Eq. (7), leading to chain disentanglement. According to Eqs. (6) and (7), the critical condition is

$$f_{retract} = f_{ent}, \quad \text{i.e,} \quad \text{when } \gamma = \gamma_c \sim 1.0. \tag{8}$$

A similar criterion can be derived using an energy argument: An instant external deformation stores elastic energy in an entangled system, amounting to raising its free energy or causing the system to lose entropy so that the chains can feel free to disentangle.[58] Figure 9 depicts the consequence of having a sufficiently high retraction force: chain disentanglement. Perhaps future studies could attempt to answer the question of whether such chain disentanglement would produce transiently enhanced flow birefringence upon step shear.

According to this criterion of Eq. (8), the cohesion due to chain entanglement is exceeded at a critical strain that is essentially independent of the level of chain entanglement, Z. Since a similar condition can be obtained for extension, we have anticipated and found[44] that an entangled melt under uniaxial extension also suffers breakup in the form of necking after a sudden stretching beyond a critical strain. The cohesive failure indeed occurs[44] at the same critical level of stretching for five melts of different levels of entanglement with Z ranging from 24 to 160.

For completeness, it is perhaps necessary to acknowledge that for the condition of Eq. (8) to produce chain disentanglement, the available force $f_{retract}$ per strand must also overcome a frictional force f_R associated with a rapid disentanglement process. Being frictional in nature, $f_R \approx \zeta N_e V$, with ζ being the segmental friction coefficient and V is the speed with which a chain retracts in space during disentanglement. It is reasonable to expect the disentanglement process to involve a time scale on the order of the Rouse relaxation time τ_R. Therefore, we have $V = L/\tau_R$, where L is the contour length and τ_R is related to the coil size as $\tau_R \sim R_g^2/(k_BT/\zeta N)$. We thus find $f_R \approx k_BT(L/R_g^2)/Z \sim (k_BT/l_{ent})/Z$, which is only $1/Z$ times the available retraction force $f_{retract}$ at the disentanglement condition of $\gamma_c = 1$ and thus negligible for well-entangled systems with $Z \gg 1$.

B. Yield behavior in continuous deformation: Stress overshoot and force imbalance

The most common procedure of imposing an external deformation involves either imposing, at $t=0$, a constant velocity V on one of two parallel surfaces separated by a gap H (to produce shear deformation) or constant velocity $\pm V$ on respective ends of a specimen at a fixed length L (to produce uniaxial extension). If the rate $\dot{\gamma} = V/H$ or $\dot{\varepsilon} = V/L$ is high enough relative to the terminal relaxation rate $1/\tau$, each chain in an entangled polymer may initially suffer affine deformation.

As indicated in Eq. (3), the force Σ that is measured in a standard shear or extension experiment (with $\dot{\gamma}$ or $\dot{\varepsilon} \gg \tau^{-1}$) arises from entropic resistance by all strands against the imposed deformation. Initially, chain deformation grows monotonically in time along with the imposed external deformation γ or ε, producing the bonded forces in each chain. So the measured stress also grows in time, as seen in Figs. 3 and 5, reflecting the increase of the bonded forces. For convenience of discussion, we summarize the experimentally observed characteristics in Figs. 10 and 11 for three different shear rates in two different representations. In time, the measured force $\Sigma = \sigma A_0$ reaches a maximum, i.e., a yield point emerges at t_{max} or γ_y. The character of this yield point is the subject of Secs. IV B 2 and IV C.

1. Intermolecular locking force f_{iml}

In search of basic ingredients in a more realistic physical picture, we ask what causes a given test chain or the strands along it to undergo conformational deformation. Consider a test chain in a monodisperse entangled melt[59] that is undergoing a sudden uniaxial extension. This chain, as a fractal object with dimensionality 2, has its pervaded volume filled up by many other chains according to the packing model for entanglement.[28] It gets stretched due to its intimately intertwining contacts with the surrounding coiled chains that are also undergoing deformation. Thus, as far as this test chain or its strands are concerned, there are external forces exerted on the test chain at the entanglement junctions, as elucidated in Fig. 12. We call these nonbonded forces *intermolecular*

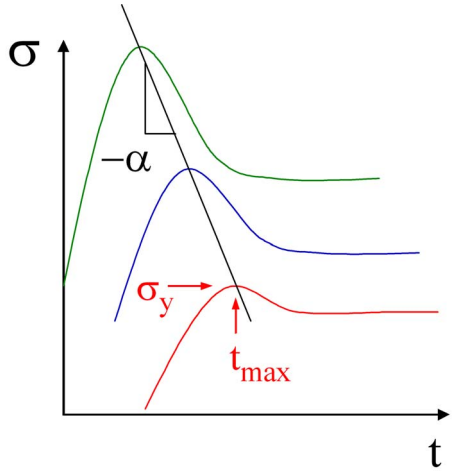

FIG. 10. (Color online) Depiction of force growth (double-log scale) during continuous deformation at three rates. At the yield point, the peak stress σ_y scales with time as $\sigma_y \sim (t_{max})^{-\alpha}$ according to the actual experimental data from Figs. 3 and 5.

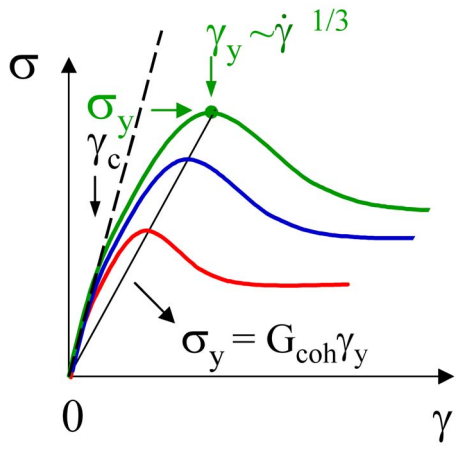

FIG. 11. (Color online) Stress growth as a function of strain on linear scale, where γ_c appears to be around unity, coinciding with the critical strain for a strained sample to break up during relaxation as discussed in Section II A. The observed linear relationship between σ_y and γ_y at the yield point introduces a cohesive modulus G_{coh} that is actually found (Refs. 52 and 53) to be of the same order of magnitude as the elastic plateau modulus G_p.

locking force f_{iml}. This kind of force originates from the imposed deformation. In a macroscopic deformation experiment, f_{iml} produces chain deformation and the corresponding bonded retraction force $f_{retract}$. Before reaching the point of yield or force imbalance, the nonbonded force f_{iml} is constantly balanced by the bonded $f_{retract}$. Thus, the measured total force or stress grows as depicted in Fig. 10 or 11. We illustrate in Fig. 12 the three forces that play active roles in the process of an entangled polymer undergoing deformation first and subsequently facing the possibility of force imbalance. When $f_{iml} < f_{retract} - f_{ent}$, disentanglement may occur during flow. For continuous flow, how this condition is met will be discussed below. In the case of interrupted deformation, the disentanglement condition is readily met as the flow cessation turns f_{iml} off, leading to the criterion given in Eq. (8). In other words, the step deformation is a special case of the continuous deformation, involving only the two forces instead of all three. More importantly, a force imbalance, i.e., $f_{retract} > f_{ent}$, can occur at a significantly lower strain after step deformation.

2. Imbalance of forces at yield point

It is reasonable that during a startup continuous deformation, f_{iml} is initially of a high magnitude as all the chains are locked into their intertwining relationship. This initial "glassy" response is not observable from the stress $\sigma = \Sigma / A_0$ because the measured σ is initially quite small according to Eq. (3) as γ is small initially. The glassy behavior can be illustrated by examining $G(t) = \sigma(t)/\gamma(t)$ in a startup shear that shows typical glass-rubber transitional behavior at short times, with $G(t) \sim t^{-1/2}$. Over time, the effectiveness of the interchain locking declines as the gripping of the red test chain by other chains (represented by blue "rings" in Fig. 12) gets loose due to the concurrent segmental relaxation. In other words, f_{iml} is expected to decline. No theory is available to relate the time dependence of $f_{iml}(t)$ to the deformation history and chain relaxation processes. The best indirect evidence for the decline of $f_{iml}(t)$ with time is the occurrence of the force maxima observed for both shear and extension in Figs. 3 and 5, where the measured stress declines in time after the point of yield at (γ_y, σ_y) depicted in Fig. 11 before inhomogeneous flow is observed.

In contrast to the declining f_{iml}, the retraction force $f_{retract}$ monotonically increases as the elapsed strain γ or ε grows linearly in time at a fixed rate until the declining f_{iml} can no longer sustain further chain deformation. Once built up, $f_{retract}$ would not relax until $t \sim \tau$, whereas the available level of f_{iml} continues to drop in time. As long as $f_{retract}$ is balanced by f_{iml}, there cannot be disentanglement thanks to the presence of f_{ent}, as illustrated in Fig. 12. Eventually, a force imbalance is bound to occur, as depicted in Fig. 13 for three different rates.

The decline of f_{iml} is an in evitable consequence of segmental relaxation dynamics. At a time t comparable to the Rouse relaxation time τ_R, fast local conformational relaxation begins to occur in spite of chain entanglement. This would reduce the effectiveness of f_{iml} to produce chain deformation leading to a slowing down of the monotonic increase of $f_{retract}$. Another scenario would be that the force imbalance occurs progressively because the entanglement network is inherently inhomogeneous, leading to the deviation of the measured force from linear growth. A force maximum is passed when the rate of losing entanglement due to the individual force imbalance events overwhelms the growing $f_{retract}$ of the remaining entanglements. The wide separa-

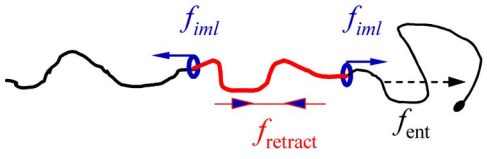

FIG. 12. (Color online) Depiction of continuous uniaxial extension, where the entangled strand between the two "rings" near the chain end is shown to undergo stretching, due to f_{iml} at the entanglement junctions (open rings), leading to $f_{retract}$. Removal of this entanglement requires straightening the dangling strand on the right-hand side of the junction. In other words, there is a force of f_{ent} resisting dissolution of the entanglement point.

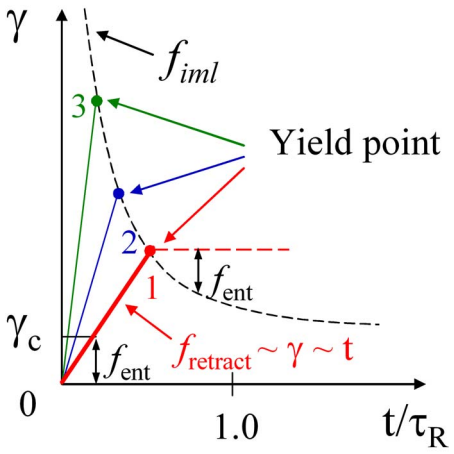

FIG. 13. (Color online) Force imbalance at the yield point between the monotonically growing retraction force f_{retract} and the declining driving force f_{iml}, for three different rates of deformation that introduce three different experimental time scales.

tion of time scale between τ_R and τ (by a factor of $Z = M/M_e \gg 1$) for well-entangled polymers ensures occurrence of force imbalance and elastic breakup of the deformed entanglement network. Other effects such as constraint release might further assist the disentanglement process leading potentially to inhomogeneous deformation.

In both step strain and continuous deformations, it is the same retraction force f_{retract}, originating from the chain deformation imposed by the sudden external deformation, that overcomes the entropic cohesion of the entanglement network and produces chain disentanglement. In the case of step strain, as indicated in Fig. 11, the critical external deformation γ_c around 1.4 can be much lower than the yield point γ_y, which grows with the shear rate as $\gamma_y \sim \dot{\gamma}^{1/3}$, as indicated in the inset of Fig. 4. A much lower value of f_{retract} is sufficient to break up the entanglement network because after shear cessation it only needs to exceed f_{ent}. In contrast, during continuous deformation, f_{iml} is also present to balance f_{retract} until the yield point at a strain γ_y of shear or ε_y of extension. This explains the counterintuitive behavior that nonquiescent motions can be observed at a considerable lower level of deformation after a step strain, whereas inhomogeneous flow only occurs at a significantly high strain during continuous deformation. In other words, γ_c (or ε_c) can be considerably lower than γ_y (or ε_y). It is our assertion that both nonquiescent relaxation after interrupted deformation and nonuniform straining during continuous deformation have the same origin: elastically driven failure of the entanglement network.

C. Scaling behavior in elastic deformation regime: $\dot{\gamma}\tau_R$ or $\dot{\varepsilon}\tau_R > 1$

The recent strain recovery experiments for both shear[52] and extensional[53] deformations revealed complete strain recovery up to the yield point, in the elastic deformation regime defined by $\dot{\gamma}\tau_R$ or $\dot{\varepsilon}\tau_R > 1$. At present, there is no theoretical account of f_{iml} as a function of time t and applied rate of deformation. We have speculated and postulated that f_{iml} is a decreasing function of time for any given value of $\dot{\gamma}$ or $\dot{\varepsilon}$, which primarily controls how quickly the retraction force f_{retract} builds up in time. In the absence of a multiple-chain statistical mechanical theory for dynamics of entangled polymers, we take a primitive approach by assuming the following scaling decay for the intermolecular locking force

$$f_{\text{iml}}(t) \sim t^{-\alpha}. \tag{9}$$

At the yield point depicted in Figs. 10 and 11 when the force imbalance occurs and the chain deformation ceases to increase, we have

$$f_{\text{iml}}(t_{\max}) = f_{\text{retract}}(\gamma_y). \tag{10}$$

Inserting Eqs. (6) and (9) into Eq. (10), we have

$$\gamma_y \sim \dot{\gamma}^{\alpha/(1+\alpha)}, \tag{11}$$

where use was made of the kinematic relation $t_{\max} = \gamma_y/\dot{\gamma}$. Thus, from the notion of force imbalance at the stress overshoot, we can learn about the conjectured time dependence of the intermolecular locking force $f_{\text{iml}}(t)$ by probing how γ_y at the stress maximum scales with the applied shear rate $\dot{\gamma}$. As sketched in Fig. 11, the startup continuous shear experiments reveal $\gamma_y \sim \dot{\gamma}^{1/3}$, as shown Fig. 4. Therefore, we have $1/3 = \alpha/(+\alpha)$, leading to $\alpha = 1/2$ in Eq. (9), which is indeed borne out in the experimental data of Figs. 3 and 5 for both continuous shear and extension. Moreover, the yield stress is then found to scale with the applied rate with exponent 1/3: $\sigma_y \sim \gamma_y \sim \dot{\gamma}^{1/3}$, in contrast to the logarithmically weak dependence of yield stress associated with deformation of glasses, although it was pointed out before that deformation of melts should resemble that of glassy polymers.[60] In fact, the proper analogy of yielding of glassy materials is the brittle failure of entangled polymeric liquids at higher rates of deformation, which is a subject just beyond the scope of the current topic.

From an experimental standpoint, the scaling exponent 1/3, as seen in Fig. 4, is a necessary consequence of both the scaling law of Eq. (9) with $\alpha = /2$, as revealed in Figs. 3 and 5, and the linear scaling of Eq. (6), as disclosed in Fig. 4 and sketched in Fig. 11. From a theoretical viewing angle, scaling behavior of Eq. (9), along with Eq. (6), would also be a sufficient condition for the scaling law of Eq. (11). It is intriguing to recognize that the value of exponent α, 1/2, is indicative of the quiescent Rouse chain relaxation dynamics of entangled polymers at short times.

We can also derive an auxiliary scaling relationship that characterizes how $t_{\max}$ varies with the shear rate $\dot{\gamma}$. Since $t_{\max} = \gamma_y/\dot{\gamma}$, Eq. (11) reveals

$$t_{\max} \sim \dot{\gamma}^{-2/3}, \tag{12}$$

for $\alpha = 1/2$. Along with Eq. (11), Eq. (12) describes how the coordinate γ_y or $t_{\max}$ of the yield point depends on the shear rate $\dot{\gamma}$ in the elastic deformation regime. Note that the Doi-Edward tube theory also predicts a shear stress overshoot based on calculation of the bonded force as a result of chain retraction.[12] Specifically, the characteristics of the stress maximum is described by $\dot{\gamma}t_{\max} \sim 2.0$, i.e., $t_{\max} \sim \dot{\gamma}^{-1}$, which amounts to setting $\alpha = 0$. In the DE theory, the concept of f_{iml} does not enter into consideration. It might be reasonable to think that f_{iml} is implicitly independent of time in the DE theory. More seriously, the decline of shear stress with time beyond the maximum is due to the chain retraction in the DE

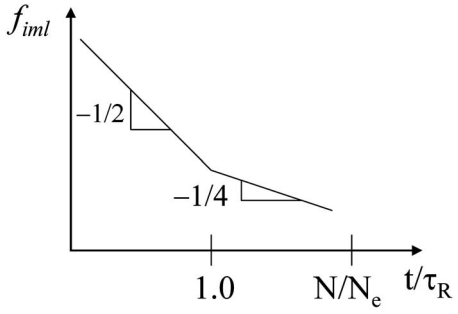

FIG. 14. Conjectured scaling behavior of the intermolecular locking force f_{iml} as a function of the rescaled time by τ_R so that the dimensionless terminal relaxation time τ/τ_R is $Z=N/N_e$.

theory, whereas we perceive the overshoot as the point of yield and force imbalance, beyond which cohesion due to entanglement would be overcome. In other words, the number of entanglements per chain would substantially decrease beyond the yield point in our theoretical picture of the stress overshoot. In experiment, the overshoot in well entangled polymers is associated with emergence of inhomogenous flow.[40] On the contrary, the original DE theory assumes the tube diameter to be constant independent of $\dot{\gamma}$. The more recent version also assumes the entanglement spacing to be constant.[7] In this case, it appears to us that the current tube theory can not anticipate any inhomogeneous shear, in contradiction with the experimental observations.[13,14,40]

D. Scaling behavior in viscoelastic deformation regime: $\tau_R^{-1} > \dot{\gamma}$ or $\dot{\varepsilon} > \tau^{-1}$

When the applied rate of deformation is lower, i.e., below the reciprocal τ_R yet still above the reciprocal quiescent terminal relaxation time τ, the exponent in Eq. (9) is experimentally found to be different, as shown in Fig. 3. In this viscoelastic regime defined by $\tau_R^{-1} > \dot{\gamma}$ or $\dot{\varepsilon} > \tau^{-1}$, the time taken to undergo 100% deformation is longer than τ_R. Thus, during deformation, considerable relaxation of local chain conformations is in competition with the continuing chain deformation. As a result, the effectiveness of the nonbonded intermolecular locking interactions to produce net chain deformation is further reduced. Naturally, the force imbalance between f_{retract} and f_{iml} occurs at a lower force maximum. More importantly, instead of expecting f_{iml} to decrease with time as $t^{-1/2}$ according to Rouse dynamics, we may actually expect the decline of f_{iml} at longer times to be more gradual because f_{iml} should eventually approach a constant in time. Experiments revealed a $-1/4$ scaling law, as shown in Fig. 3 and elsewhere,[52] suggesting $f_{\mathrm{iml}} \sim t^{-/4}$ for $t > \tau_R$, as depicted in Fig. 14. We note that the scaling exponent changing from $-1/2$ to $-1/4$ mirrors the scaling behavior of segmental displacement in quiescence, as given in Fig. 6.10 of Ref. 6. The recent strain recovery experiments for both shear[52] and extensional[53] deformations indicate that in this viscoelastic regime considerable flow occurs beyond the force maximum. It is clear that the decline of the measured force after the overshoot is still a result of force imbalance, and the action of f_{retract} is to cause chain disentanglement that may lead to inhomogeneous shear.[40,45] Since f_{iml} is declining less sharply in this viscoelastic regime, as depicted in Fig. 14, the development of the force imbalance is less dramatic. Also less drastic are the events of chain disentanglement, which are borne out by experiments showing the drop of the measured force on a much longer time scale at a lower applied rate.

E. Terminal flow regime: $\dot{\gamma}\tau$ or $\dot{\varepsilon}\tau < 1$

Finally, we shift attention to the terminal regime where the experimental time scale, characterized by $\dot{\gamma}^{-1}$ or $\dot{\varepsilon}^{-1}$, is longer than the terminal relaxation time τ. In this regime, chain diffusion and relaxation through reptationlike and nonreptative motions are a dominant factor. Since the external deformation is imposed so slowly relative to the chain dynamics, chains cannot be effectively deformed. Consequently, the retraction force f_{retract} only gradually approaches its steady state value determined by the nonbonded interchain viscous interactions. Actually, a startup continuous deformation in this regime does not result in any stress overshoot, and only smooth homogeneous flow takes place. Similarly, in a step strain, there is not sufficient residual retraction force to overcome the cohesive entanglement force, and the relaxation does proceed *quiescently*. Indeed, recent experiments based on PTV observations[13,14,40] support these expectations. In other words, terminal flow behavior is linearly viscoelastic and can be understood more straightforwardly.

As long as the retraction force is insufficient to overcome cohesion due to chain entanglement, it is plausible to consider the chain dynamics localized by an effective potential such as a tube in a Doi-Edwards-type model. On the other hand, we note the continuing debate[8,36,38,39] about whether this single-chain picture involving evaluation of only bonded forces is adequate or not for depicting LVE of entangled polymers, as discussed in Sec. II.

V. CONCLUSIONS

Recent experimental observations of inhomogeneous flow have provided valuable clues about what to expect from entangled polymers under externally imposed deformation. In particular, they have revealed essential ingredients that must be present in a new theoretical description of polymer rheology. The theoretical considerations in this paper attempted to provide a plausible picture of what actually is going on in flow of well-entangled polymers. Although the current scaling treatments are at a single-chain level, they have already provided a useful guideline and have even allowed us to anticipate two unexpected phenomena, as described in Fig. 2(c), and arrested wall slip.[61]

The experimental message of inhomogeneous structural breakup also provides a working guideline for studying nonlinear flow behavior of other complex fluids including associative polymers, concentrated emulsions and blends, wormlike entangled micellar solutions, gels, foams, and many yield-stress materials. Although these complex fluids may display similar phenomenology such as yieldlike characteristics leading to inhomogeneous flow, the specific physics is different in each case.

In the case of well-entangled polymers, we have identified three forces and their roles in influencing the experimentally observed cohesive failures in both step and continuous deformations. The very existence of these forces, the nonbonded intermolecular locking force f_{iml}, the elastic retraction force f_{retract}, and the cohesive entanglement force f_{ent}, and their effects on molecular events that can take place during rapid large deformation appear to have been overlooked and underappreciated in the past. In our perception and definition, the nonbonded f_{iml} is zero in quiescence and is solely due to external deformation that displaces each chain according to deformation kinematics, whereas f_{ent} symbolizes the cohesive strength of the network due to chain entanglement. It is due to f_{ent} that an entangled polymer appears to be a solid of modulus G_p on a time scale shorter than the quiescent terminal relaxation time τ. The essence of f_{ent} can be further examined from a stress relaxation experiment in the linear regime: Upon flow cessation, f_{iml} vanishes immediately. The residual stress due to the bonded retraction forces is present because it is balanced by f_{ent}, which can be thought of also as *nonbonded* forces that prevent the sample from flowing in the presence of the residual stress. It is our contention that a time-sensitive imbalance among these forces is at the origin of the observed yielding of entangled polymers through chain disentanglement. This breakdown of the entanglement network occurs at a lower strain upon interruption of deformation than during continuous deformation. A heuristic cartoon has been suggested in Fig. 12 that summarizes the essence of our theoretical investigation, depicting the relationship among the three forces in the example of uniaxial extension.[44,53]

We have identified three regimes of different responses that depend on the rate of external deformation. In the elastic deformation regime accessible by having $\dot{\gamma}\tau_R$ or $\dot{\varepsilon}\tau_R > 1$, specific scaling behavior is found: the force at the yield point scales linearly with the elapsed strain γ_y, and γ_y scales to the $1/3$ power of the shear rate $\dot{\gamma}$, as revealed in Fig. 4. We have indicated that the scaling $\gamma_y \sim \dot{\gamma}^{1/3}$ might be understood in terms of a force imbalance, $f_{\mathrm{iml}}(t) < f_{\mathrm{retract}}(\gamma)$, with the driving force $f_{\mathrm{iml}}(t)$ declining as $t^{-1/2}$. In the crossover viscoelastic regime defined by $\tau_R^{-1} > \dot{\gamma}$ or $\dot{\varepsilon} > \tau^{-1}$, force imbalance is also responsible for the occurrence of a force maximum, leading to subsequent significant flow deformation. It appears that $f_{\mathrm{iml}}(t) \sim t^{-1/4}$ in this regime. The terminal flow regime is of course well known and reasonably well understood by conventional considerations.

Under conditions described in this paper, we have encountered ductile yieldlike failure that has been theoretically identified as due to the internal elastic force overcoming the cohesion of chain entanglement. A brittle rupture of entangled polymers that occurs at higher rates of deformation is a topic beyond the scope of the present work. Also left for future work is the brittle fracture that can take place under the influence of a constant external force.

In summary, we have been carrying out an integrated research program of both experimental and theoretical characters to move forward in search of a more realistic description of polymer flow. We are clearly at the very beginning of such an effort. Nevertheless, there is a sense of new optimism. On the experimental side, we anticipate a great deal more to be learned about *melt* flow behavior in both shear and extension, although the initial results, including those presented in Figs. 2(b) and 2(c), are in accord with those learned from entangled solutions. On the theoretical side, a major task is to develop a detailed microscopic theory that could describe how f_{iml} explicitly depends on time, rate of deformation, and chain deformation in the presence of chain relaxation, and whether there is any validity of the scaling law hypothesized in Eq. (9) and Fig. 14. This appears to be a first step toward a first-principles theory capable of describing the yield criterion for entangled polymers under external deformation.

In short, one needs to first ask whether entangled polymers are able to flow smoothly without inhomogeneous cohesive breakdown. For well-entangled polymers, there is a wide separation of time scales because the ratio of the terminal relaxation time τ to the Rouse relaxation time τ_R given by $Z = M/M_e$ is large. This question becomes less acute for moderately entangled polymers because these polymers may access more readily the faster relaxation of Rouse motion, with τ approaching τ_R. For $Z \gg 1$, inhomogeneous flow appears to be the norm rather than exception in startup flow in the stress plateau region. Our first task should be to describe the onset condition for yielding that leads to inhomogeneous flow, which is a much more modest goal than that of formulating a constitutive relationship, which seems rather formidable at this moment. The detailed dynamics governing chain disentanglement and how disentanglement instability develops in a macroscopic system are further and more challenging topics waiting to be addressed in the future by both experiment and theory. We hope that molecular dynamics computer simulations could help us in the near future to further visualize and quantify the nature and characteristics of the various forces that control the responses of chain entanglement network in flow.

ACKNOWLEDGMENTS

The current version represents great improvement over a previous one as a result of addressing a comment by P. G. de Gennes on an earlier draft of this manuscript about whether chain entanglement really provides a cohesive force that holds up an entangled polymer as a solid on time scales much shorter than the quiescent terminal relaxation time. One of the authors (S.-Q.W) also acknowledges useful conversations with K. Schweizer, A. Gent, and J. Douglas. This work is supported, in part, by a Small Grant for Exploratory Research of the National Science Foundation (DMR-0603951) and an ACS grant (PRF No. 40596-AC7). This paper is dedicated to the memory of Pierre-Gilles de Gennes.

[1] F. Bueche, *Physical Properties of Polymers* (Wiley, New York, 1962).
[2] W. W. Graessley, Adv. Polym. Sci. **16**, 1 (1974).
[3] J. D. Ferry, *Viscoelastic Properties of Polymers*, 3rd ed. (Wiley, New York, 1980).
[4] M. S. Green and A. V. Tobolsky, J. Chem. Phys. **14**, 80 (1946).
[5] P. G. de Gennes, J. Chem. Phys. **55**, 572 (1971).
[6] M. Doi and S. F. Edwards, *The Theory of Polymer Dynamics*, 2nd ed. (Clarendon, Oxford, 1988).

[7] R. S. Graham, A. E. Likhtman, T. C. B. McLeish, and S. T. Milner, J. Rheol. **47**, 1171 (2003).
[8] M. Fuchs and K. S. Schweizer, Macromolecules **30**, 5133 (1997); **30**, 5156 (1997); K. S. Schweizer, M. Fuchs, G. Szamel, M. Guenza, and H. Tang, Macromol. Theory Simul. **6**, 1037 (1997).
[9] M. Doi, J. Polym. Sci., Polym. Phys. Ed. **18**, 1005 (1980).
[10] K. Osaki, K. Nishizawa, and M. Kurata, Macromolecules **15**, 1068 (1982).
[11] S. Q. Wang, S. Ranvindranath, P. Boukany, M. Olechnowicz, R. P. Quirk, A. Halasa, and J. Mays, Phys. Rev. Lett. **97**, 187801 (2006).
[12] M. Doi and S. F. Edwards, J. Chem. Soc., Faraday Trans. 2 **75**, 38 (1979).
[13] P. Tapadia and S. Q. Wang, Phys. Rev. Lett. **96**, 016001 (2006).
[14] P. Boukany and S. Q. Wang, J. Rheol. **51**, 217 (2007).
[15] G. Ianniruberto and G. Marrucci, J. Non-Newtonian Fluid Mech. **65**, 241 (1996).
[16] D. W. Mead, R. G. Larson, and M. Doi, Macromolecules **31**, 7895 (1998).
[17] G. Ianniruberto and G. Marrucci, J. Non-Newtonian Fluid Mech. **95**, 363 (2000).
[18] S. T. Milner, T. C. B. McLeish, and A. E. Likhtman, J. Rheol. **45**, 539 (2001).
[19] G. Marrucci and G. Ianniruberto, Philos. Trans. R. Soc. London, Ser. A **361**, 677 (2003).
[20] G. Marrucci, J. Non-Newtonian Fluid Mech. **62**, 241 (1996).
[21] J. F. Douglas and J. B. Hubbard, Macromolecules **24**, 3163 (1991).
[22] H. Mendil, P. Baroni, and L. Noirez, Eur. Phys. J. E **19**, 77 (2006).
[23] M. Guenza, Phys. Rev. Lett. **88**, 025901 (2002).
[24] R. H. Colby, D. C. Boris, W. E. Krause, and S. Dou, Rheol. Acta **46**, 569 (2007).
[25] S. Q. Wang, J. Polym. Sci., Part B: Polym. Phys. **41**, 1589 (2003).
[26] L. J. Fetters, D. J. Lohse, S. T. Milner, and W. W. Graessley, Macromolecules **32**, 6847 (1999).
[27] N. Heymans, Macromolecules **33**, 4226 (2000). This article reviewed most of available theoretical models on the subject of chain entanglement.
[28] Y.-H. Lin, Macromolecules **20**, 3080 (1987).
[29] T. A. Kavassalis and J. Noolandi, Macromolecules **59**, 2674 (1987); **21**, 2869 (1988); **22**, 2709 (1988).
[30] L. J. Fetters, D. J. Lohse, D. Richter, T. A. Witten, and A. Zirkel, Macromolecules **27**, 4639 (1994).
[31] L. J. Fetters, D. J. Lohse, and W. W. Graessley, J. Polym. Sci., Part B: Polym. Phys. **37**, 1023 (1999).
[32] In Ref. 28, Q_e was taken to be 2. However, based on the data provided in the same paper, we see that the majority of data yield a value for Q_e between 5 and 6. See Ref. 34.
[33] R. P. Wool, Macromolecules **26**, 1564 (1993).
[34] S. Q. Wang, Macromolecules (to be published).
[35] H. M. James and E. Guth, J. Chem. Phys. **11**, 455 (1943).
[36] M. Fixman, J. Chem. Phys. **95**, 1410 (1991).
[37] J. Gao and J. H. Weiner, Macromolecules **24**, 5179 (1991).
[38] A. F. Bower and J. H. Weiner, J. Chem. Phys. **118**, 11297 (2003).
[39] J. Ramírez, S. K. Sukumaran, and A. E. Likhtman, J. Chem. Phys. (to be published).
[40] S. Ravindranath and S. Q. Wang, Macromolecules (to be published).
[41] Chain retraction was perceived in the DE tube theory to occur on a time scale around the Rouse relaxation time τ_R when a sudden external deformation (taking place on a time scale shorter than τ_R) has caused the primitive chain to deform affinely beyond its equilibrium contour length. This retraction causes the chain to return to its equilibrium length. It is also this process that gives rise to the kinklike decline in the Doi-Edwards theory, as depicted in Fig. 1, and led to the nonmonotonic relation of $\bar{\sigma}(\gamma)$ versus γ as discussed in the Introduction. However, the chain retraction, predicted to take place after a large step strain in the DE theory, does not lead to the primitive chain leaping out of the tube, resulting in disentanglement.
[42] M. E. Cates, T. C. B. McLeish, and G. Marrucci, Europhys. Lett. **21**, 451 (1993).
[43] S. Ravindranath and S. Q. Wang, Macromolecules (to be published).
[44] Y. Wang, S. Q. Wang, P. Boukany, and X. Wang, Phys. Rev. Lett. (submitted).
[45] P. Boukany and S. Q. Wang (unpublished).
[46] J. D. Huppler, I. F. Macdonald, E. Ashare, T. W. Spriggs, R. B. Bird, and L. A. Holmes, Trans. Soc. Rheol. **11**, 181 (1967).
[47] R. L. Crawley and W. W. Graessley, Trans. Soc. Rheol. **21**, 19 (1977).
[48] E. V. Menezes and W. W. Graessley, J. Polym. Sci., Polym. Phys. Ed. **20**, 1817 (1982).
[49] C. Pattamaprom and R. G. Larson, Macromolecules **34**, 5229 (2001).
[50] P. Tapadia and S. Q. Wang, Macromolecules **37**, 9083 (2004).
[51] It is crucial to note that since shear deformation involves an unchanged area of the sample, we can freely choose either the total shear force or the normalized force, i.e., shear stress to quantify the phenomenon. For extension, a distinction must be made (Ref. 53) between engineering stress denoting the total tensile force for elastic extension and true stress that is a quantity only to be used to depict extensional flow.
[52] S. Ravindranath and S. Q. Wang, J. Rheol. (to be published).
[53] Y. Wang and S. Q. Wang, J. Rheol. (to be published).
[54] W. W. Graessley and S. F. Edwards, Polymer **22**, 1329 (1981).
[55] S. Wang, S. Q. Wang, A. Halasa, and W.-L. Hsu, Macromolecules **36**, 5355 (2003).
[56] S. Glasstone, K. J. Laidler, and H. Eyring, *The Theory of Rate Processes* (McGraw-Hill, New York, 1941).
[57] P. G. de Gennes, J. Phys. (Paris) **36**, 1199 (1975).
[58] Take step shear, for example. The external work per unit volume done during an affine elastic deformation is given by $w=\frac{1}{2}\sigma\gamma$, where $\sigma=G_p\gamma$ with G_p given by Eq. (5). This stored elastic energy $E_{\mathrm{el}}=w$ per unit volume is available to pay for entropy loss on the order of k_BT for each strand involved in disentanglement. Since the number of strands per unit volume is $\phi\rho N_a/M_e(\phi)$, we can equate E_{el} to $[\phi\rho N_a/M_e(\phi)]k_BT$ to arrive at a condition for disentanglement: $\gamma_c^2\sim 2$, i.e., $\gamma_c\sim 1.4$.
[59] If this sample's weight is $\sim$0.1 g and molecular weight $M_w=100$ kg/mol, then there are about 6×10^{17} chains in this statistical ensemble.
[60] S. Matsuoka, *Relaxation Phenomena in Polymers* (Hanser, New York, 1992).
[61] Y. Wang, P. Boukany, and S. Q. Wang, J. Rheol. (to be published). Wall slip due to disentanglement of the adsorbed chains with bulk chains also follow the discovered criteria discussed in Sec. IV B. For different entangled melts undergoing displacement-driven simple shear in a homemade parallel-plate sliding rheometer, we observed, using our particle tracking-velocimetric method, that the boundary condition would remain no slip during shear, yet massive wall slip was observed upon shear cessation, which we call "arrested wall slip." This counterintuitive phenomenon, initially anticipated by theoretical considerations reflected in Eq. (8), occurs because upon shear cessation, f_{iml} vanishes instantly so that the available f_{retract} only needs to be beyond a threshold defined by f_{ent} to produce chain disentanglement at the melt/wall interface.